Lasers in Manufacturing Conference 2021

Comparison of different density measurement techniques for laser assisted powder bed fusion

Lisa Schade[a*], Gabor Matthäus[a], Hagen Kohl[a], Roland Ramm[b] Burak Yürekli[a], Tobias Ullsperger[a], Brian Seyfarth[a,b], Stefan Nolte[a,b]

[a]*Institute of Applied Physics, Abbe Center of Photonics, Friedrich Schiller University Jena, Albert-Einstein-Straße 15, 07745 Jena, Germany.*
[b]*Fraunhofer Institute for Applied Optics and Precision Engineering IOF, Center of Excellence in Photonics, Albert-Einstein-Straße 7, 07745 Jena, Germany*

Abstract

One of the major quality control criteria for additively manufactured parts is the density achieved. Besides fundamental properties like microstructure, residual strain or impurities, the density fundamentally defines how the final product matches the intended material properties. In general, mostly surface inspections of randomly prepared cross sections are undertaken. On the one hand side, this approach delivers important information regarding the morphology and distribution of pores, however, on the other hand side, this characterization only considers a small fraction of the entire sample volume and therefore cannot reflect the true density without a significant level of uncertainty. In this work, we investigate four different measurement techniques, sizing and weighing, surface inspections, x-ray tomography and Archimedes´ principle with a focus on their advantages and disadvantages. The results show significant differences of the obtained density values with deviations in the range of several percent depending on the underlying material and sample size.

Powder bed fusion; Selective laser melting; Additive manufacturing; 3D printing; Density measurement

* Corresponding author. Tel.: +40-03641-947825; fax: +49-03641-947802.
E-mail address: lisa.schade@uni-jena.de

1. Introduction

Laser powder bed fusion (LPBF), also called selective laser melting (SLM), is one of the most established methods for additive manufacturing. With the help of a layer wise production cycle highly complex devices can be fabricated which are not possible with traditional manufacturing techniques.

The desired primary material is chosen with respect to the known properties of the bulk material. However, additively manufactures parts, especially when produced out of a powder bed run through a complex production cycle inside the LPBF machine. Depending on the powder material and occurring lack of fusion effects often densities are achieved that are significantly below the aspired values of the 100 % dense bulk counterpart. In particular, when materials are applied that exhibit extraordinary properties like copper or special aluminum alloys a lower density can dramatically alter the overall behavior like thermal or electrical performance [1-4]. Moreover, a decreased value in density often represents an increased probability of mechanical failure due to the existence of cracks and pores hidden inside the volume of the product. In this regard, the measurement of the final density is important to qualify the product in terms of reliability and specified performance.

In the field of additive manufacturing several different methods are applied to determine the density. Depending on the available equipment the spectrum ranges from simple sizing and weighing procedures to highly advanced X-ray tomography. All these methods differ in precision and measurement certainty, which moreover depends on sample size, shape and applied material.

In the presented work, four widely used density measurement techniques are compared. The following chapters include an introduction of the four methods, a comparison of the achieved results using steel samples (316L), a discussion about the individual pros and cons of the measurement techniques and a final suggestion depending on available equipment, sample dimensions, overall porosity and material.

2. Sample fabrication and preparation

The comparison of different density measurement techniques was done by using stainless steel samples. For the fabrication of these samples a self-developed laser powder bed fusion system was used. In contrast to conventional LPBF-machines, here, an ultrashort pulses laser serves as fusion source. The laser from active fiber systems (AFS) delivered pulses with a pulse duration of 500 fs at a central wavelength of 1030 nm. The laser beam was focused on the powder bed by using a 160 mm f-theta-objective yielding a spot diameter of 30 µm ($1/e^2$). During laser processing, the average power was set to the highest available output of 32 W (measured at powder surface) at a pulse repetition rate of 20 MHz. With a scan velocity of 100 mm/s and a hatch distance of 45 µm each layer was processed with two perpendicular hatch orientations (“cross-hatching”). The used 316L steel powder from TLS Technik exhibited spherical particles with a diameter distribution between 10 µm and 45 µm.

Fig. 1 shows typical test bodies with a size up to 1 cm^3 which were fabricated on a building platform (steel, 316L). Before the density measurements can be applied, the samples were separated from the building platform and traces from the support structure were removed using a lathe (see Fig. 1 b). For the analysis of the micrograph the parts were additionally polished. Fig. 1 c) – d) gives an impression of the surface qualities achieved. On the sample top side melt tracks are visible and a ripple structure is present (Fig. 1 c). The side walls of the test bodies exhibit melt beads and sintered powder particles (Fig. 1 d). The surface morphology has a significant influence on the characterization method. This effect will be discussed in the next section.

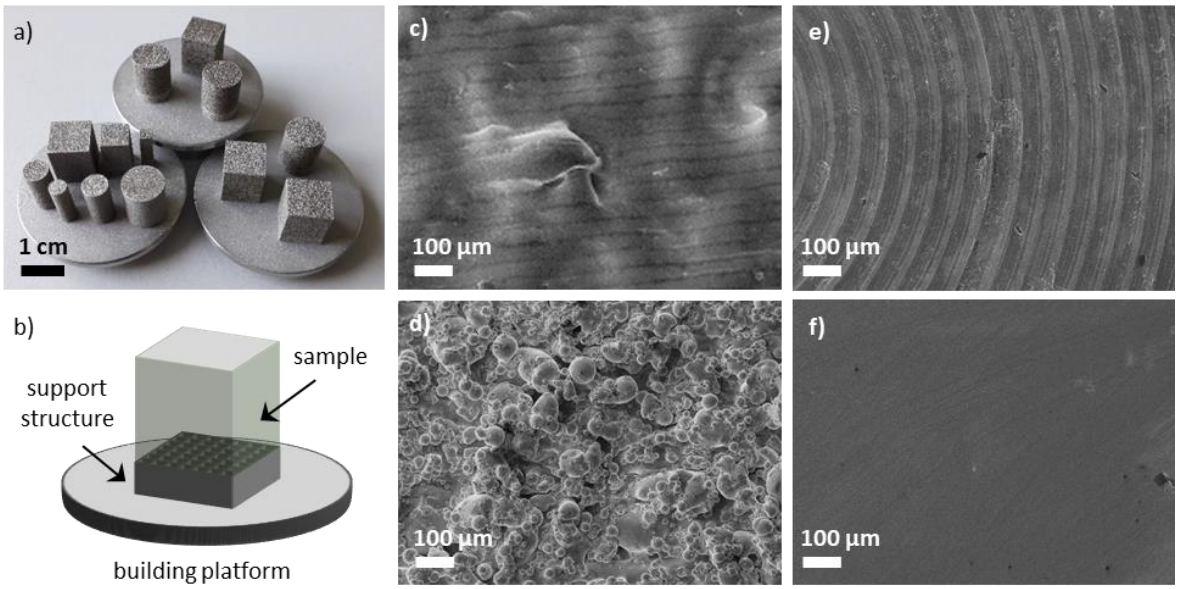

Fig. 1 a) LPBF steel parts. b) Schematic of a test body fabricated support structure beneath. c) – f) REM images of different sample surfaces: c) top layer as-built d) side wall as-built and machined bottom layer: e) raw cut and d) polished.

3. Density determination and Results

In general, the density of the samples is indicated by the filling factor ρ_{rel}. Here, the filling factor, also called relative density is the density of the sample ρ_{sample} normalized to the density of steel 316L ($\rho_{316\mathrm{L}} = 7.99\ \mathrm{g/cm^3}$).

$$\rho_{\mathrm{rel}} = \frac{\rho_{\mathrm{sample}}}{\rho_{316\mathrm{L}}} \qquad (1)$$

All given errors are absolute errors with the unit % (unit of filling factor). Therefor these values should not be mistaken as relative error of the density ρ_{sample}.

3.1. X-ray computer tomography

X-ray computer tomography (X-ray CT) is probably the most advanced way to investigate the density of workpieces. This method not only reveals the density indirectly, but it also provides important insight into the hidden inner structure of the sample yielding information about the distribution and size of pores without destroying the specimen. However, depending in the aimed resolution and sample size, this measurement technique is very time consuming (several hours per sample) and easily produces several Gbytes of data.

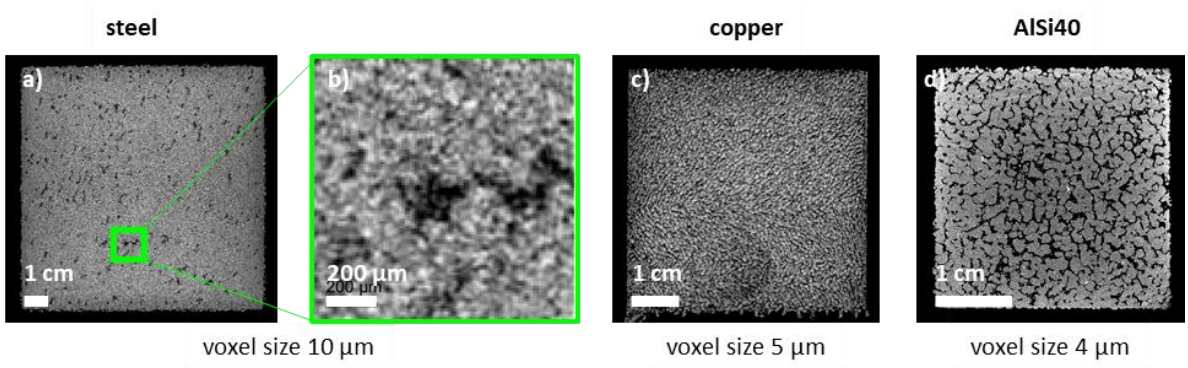

Fig. 2 X-ray computer tomography of different cross sections: a) & b) steel, c) copper and d) AlSi40.

During our investigations x-ray CT was applied using a phoenix x-ray v|tome|x operating at highest resolution settings. Hence, a cubic sample with an edge length of 1 cm delivered a voxel size of 10 µm^3. An example cross section of a steel cube is shown in Fig. 2 a). As one can see, the enlarged view in Fig. 2 b) is affected by strong background noise. The reason for the low signal to noise ratio (SNR) is the strong absorption of steel within the x-ray range and the low x-ray power usage, which is needed for best resolution. In the case of smaller sample sizes, the SNR can be increased, but in this case the sample dimensions are too small for the comparative analysis presented here. The strong material dependencies of the final resolution achieved is typical for X-ray CT and should be emphasized. Another example where larger samples cannot be measured is pure copper as seen in seen Fig. 2 c).

However, in the case of aluminum-based alloys, which are widely used in the LPBF community, X-ray CT is a convenient characterization method. Here, the measurement delivers high-contrast images where the border between material and pores is clearly visible and the determination of the filling factor out of a previously performed correlation between surface density and a few randomly taken cross sections can easily be done (see Fig. 2 d).

3.2. Sizing and weighing

An intuitive method to measure the filling factor is simple sizing and weighing of the samples if the specimen is based on a simple geometry like a cuboid or cylinder. For more complex structures this technique becomes difficult and can only be performed by using more advanced sizing methods like 3D laser scanning.

In our case, simple geometries were applied and sized with a caliber at different positions. Here, the error of this measurement is governed by statistical deviation. For weighting, a precision balance (KERN PFB 300-3) with a measurement range from 1 g up to 300 g and an accuracy of 1 mg was used. In accordance with the error propagation, for a cubic sample with a volume of 1 cm^3 the filling factor revealed an error of ρ_{rel}= ± 1 %. For smaller samples, the uncertainty increases rapidly, whereas for larger samples in the range of several 10 to 100 cm^3 this measurement delivers significantly smaller errors. However, independent from the sample size, this measurement always delivers slightly reduced values due to the intrinsic surface roughness.

The assumption, that the difference Δx of measured and averaged sample size is twice the surface roughness R_a as represented in the following equation:

$$\Delta x = x_{measured} - x_{averaged} = 2 \cdot R_a \qquad (2)$$

allows an estimation of the deviation in filling factor. Some typical values for surface roughness depending on the applied post processing are given in Table 1.

Table 1. Typical values for surface roughness depending on the post-processing

Surface	R_a [µm]
top (as built)	10-100
side (as built)	25-100
sandblasted	15-50
milled, grinded	5-25
polished	0.01-1

For example, in the case of a cubic as-built sample with a size of 1 cm^3 this roughness easily causes a systematic deviation of the filling factor of about 1 % to 2 %. In other words, the real filling factor is about 1 % to 2 % higher than the real value. In general, the surface of LPBF samples is mostly treated with abrasive blasting but not grinded or polished due to time consuming reasons. Hence, in our study only as-built or sand blasted samples were used.

3.3. Pycnometer

In a comparative study of methods for the density determination also a technique based on the Archimedes' principle should be involved. One option is two measure the mass of a sample and the mass of the sample immersed in a fluid. From the difference of these masses and the corresponding fluid buoyancy the volume and therefore the density can be calculated. This can be done with commercial density determination kits available for several balances. Another method is the usage of a pycnometer. Within this study a Gay-Lussac pycnometer was used. The used pycnometer has a capacity of 100 ml and exhibits a conically tapered ground glass joints with the ISO size 19. For weighing the balance mentioned in section 3.2. was used. To determine the density three weighing steps are needed as illustrated in Fig. 3.

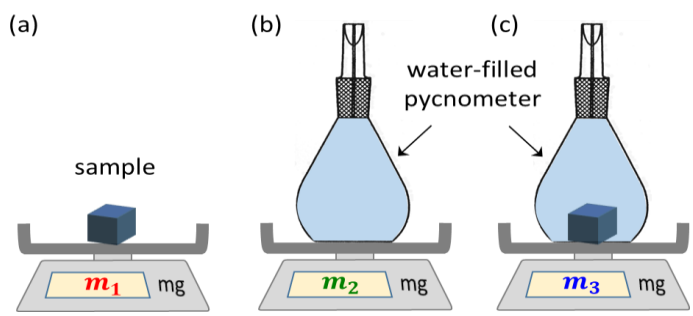

Fig. 3 Illustration of the three applied measurement steps using a pycnometer for density measurements.

First the mass of the sample m_1 is measured. Subsequently the mass of the water-filled pycnometer without and with the sample are determined (m_2 and m_3). With these masses and the known density of water ρ_{H_2O} the volume of the displace water V_{H_2O} can be calculated. Since this volume is equal to the sample volume the density can be determined by the following equation:

$$\rho_{sample} = \frac{m_1}{V_{H_2O}} = \frac{m_1 \cdot \rho_{H_2O}}{m_2 + m_1 - m_3}. \qquad (3)$$

For the weighing #2 and #3 air buoyancy must be considered. Therefor also the air pressure was detected for each measurement. All weightings were done several times at a temperature of 23 °C. The density of steel is much higher compared to the density of water, therefore variations of the water-density caused by temperature fluctuation are neglectable ($\Delta\rho_{\mathrm{rel}} < 0.05\%$).

After filling, the pycnometer was dried by wipes. During wiping with a paper towel, the glass pycnometer was charged. The resulting electric field influences the weighing. Deviations up to 400 mg were recognized, resulting in a huge variation of the filling factor. To suppress this effect the pycnometer was always measured within a metallic can, which shields the electric field.

Another error source is represented by the water film within the glass joints or the film between the opening of the flask and the stopper. For each measurement, a different amount of water is within this gap resulting in small variations of the filling factor. Therefore, each weighing was performed several times to get a statistical error for the three measured masses (see equation 3).

One has to consider, that this method is only suitable for non-porous samples or rather for samples with a closed surface, so that the water cannot flow into the sample during the measurement. In case of a porous part, where all pores can be filled with water a 100 % filling factor would be measured. To cancel out this issue the sample mass m_1 was measured again after weighing #3. During our measurements no differences could be detected, which indicate that the steel samples were suitable for the pycnometer method.

3.4. Surface density /microstructure analysis

This approach is based on the inspection of a polished surface of a randomly taken cross section. Therefore, a micrograph (light microscope image) of the polish sample surface is evaluated and the surface density is determined by the fraction between dense material and observed pores. Here the crucial point of the measurement is the definition of the correct threshold value (grayscale value), which represents the border between material and pore. Another drawback, which will be discussed later on, is the fact, that grinding the surface followed by polishing closes small pores yielding an increased density value.

A typical measurement can be seen in Fig. 4. It shows a micrograph of a polished cross section which belongs to a fabricated steel sample. An enlarged section can be seen in b) revealing a bigger pore. For demonstrating the basic analysis process two colored lines are shown in Fig. 4 c) indicating two estimated pore boundaries. For the red line, the threshold value was chosen a bit too low and for the red boundary the threshold value was taken slightly too high. As mentioned before, this reveals the major error of this measurement technique - the definition of the threshold value (gray-scale value) which is done only by personal estimation. When applying these two different threshold values (red, blue line), deviations in the filling factor of about 0.5 to 1 % are observed which is a typical result for this approach.

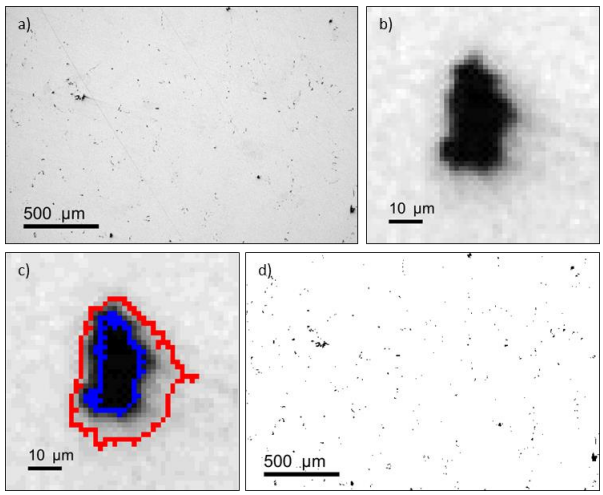

Fig. 4. a) microscope image of the polished surface of a steel test body. b) Enlarged section of a) showing a typical pore. c) blue and red lines defined as two boundary lines around the pore as an estimation for a too small and too large threshold value (grayscale value).

4. Comparison and discussion of the presented methods

In the following, the results for the filling factor of the different methods are compared. In particular, for three typical samples Table 1 shows the resulting filling factors for the sizing- and weighing (method 1), the Archimedes' principle (method 2, here pynometry) and the approach using the calculated surface density (method 3). A quantitative analysis of the X-ray CT measurement is not included, due to the high absorption inside the steel samples as discussed before. However, a qualitative analysis of several CT-images yields that many pores are randomly distributed. Hence, the filling factor cannot be close to 99 % as the surface density measurement (method 3) claims. To prove this thesis in paragraph 3.1 the X-ray CT-cross section of sample 3 is shown.

Tab. 2 Relative density (filling factor) of three different samples

sample	method 1		method 2		method 3	
	Sizing and weighing		Archimedean approach		Surface density approach	
1	91.4 %	± 0.5 %	92.3 %	± 0.7 %	99.6 %	± 0.4 %
2	94.9 %	± 0.7 %	95.4 %	± 0.6 %	99.4 %	± 0.4 %
3	93.9 %	± 0.7 %	95.7 %	± 0.6 %	99,0 %	± 1.0 %

When looking at Tab. 2, significant differences of the derived filling factors can be seen for all methods. For the same samples, the relative density ranges from ca. 91 % to above 99 %. This crucial outcome reflects one more time that reported density values or filling factors for LPBF manufactured parts must be treated critically, especially when the exact method is not mentioned or discussed in detail.

Besides this overall observation one can see, that method 1 always yields comparatively low values. This behavior was previously mentioned and is due to the measurement errors induced by surface roughness. The Archimedes' principle yields the most convincing results especially when compared to method 1 and considering the systematic errors that yields a filling factor approximately 1 % to 2 % reduced as discussed before.

Method 3 which is based on the observed surface density by using light microscopy shows always very high values in comparison to the other methods. This can be explained by several issues which are included in this method. First as mentioned before surface preparation using grinding and polishing can produce a surface that shows a significantly reduced number of pores due to dragged material inside the pores. This issue is in particular the case when ductile materials are inspected. Here pores can be closed only be deformation of the pore boundary due to pressure and the use of wearing tools. Additional sample etching or ultrasonic cleaning can help but strictly depends on the sample material.

Moreover, this method can only represent a few snap shots of the inner volume due to the fact, that just a few slices of the sample can be inspected. Often the LPBF process is characterized by inhomogeneous processing for instance due to alternating thermal coupling to the building platform or already produced parts in comparison to the weakly conducting powder bed. This becomes even more significant when complex geometries are involved.

In general, with regard to all studied methods, one has to consider, that in most cases the certainty increases when larger samples are characterized. In our measurements only samples with a volume of about 1 cm^3 were studied. However, this comparatively small volume easily reveals measurement specific drawbacks and error ranges. For a better overview all represented methods with their derived pros and cons are listed in Acknowledgements

The authors gratefully acknowledge funding by the German Research Foundation (DFG) within the Priority Program (SPP) 2122 "Materials for Additive Manufacturing (MATframe)" (grants NO462/13-1 and Re1261/23–1).

References

[1] Kaden et al., "Selective laser melting of copper using ultrashort laser pulses", Applied Physics A, 123, 596 (2017).
[2] Ullsperger et al., "Selective laser melting of hypereutectic Al-Si40-powder using ultra-short laser pulses", Applied Physics A, 123, 798 (2017).
[3] Yürekli et al., "Additive manufacturing of binary Al-Li alloys" Procedia CIRP, 94, 69-73 (2020).
[4] Kaden et al., "Additive manufacturing of pure copper using ultrashort laser pulses". Proc. SPIE 10909, Laser 3D Manufacturing VI,109090D, doi: 10.1117/12.2507401.

.

5. Conclusion

The presented work compares different density measurement methods for the characterization of additively manufactured parts using the laser powder bed fusion. These methods are sizing/weighing, X-ray tomography, Archimedes´ principle (based on pycnometry) and calculations from measured surface densities.

Our investigations reveal a huge discrepancy between the obtained results. Ranging over 5 to 10 percent depending on the porosity of the sample and sample size.

In general, all methods have their advantages and disadvantages with respect to sample geometry, size, costs, measurement times and measurement certainty. However, most certain values can be achieved by using the Archimedes´ principle as long as closed surfaces of the samples are present. Most questionable results are achieved when calculations on the surface morphology are applied. This is due to the fact, that only a few snap shots of the sample inner volume can be inspected and that surface treatment like grinding and polishing often fills previously existing pores by dragged material. This issue is in particular the case when ductile materials like copper or steel are inspected. Here pores can be closed only be deformation of the pore boundary due to pressure and the use of wearing tools.

Tab. 3 Pros and cons of studied methods for density or filling factor measurements

	X-ray CT	Sizing and weighing	Archimedes´ principle	Surface density approach
Pros	• full inside into the sample volume • distribution of pores visible • process variations, errors visible • complex shapes possible • good results for weak absorbing material	• low costs • fast • mediocre results	• low costs • fast • complex shapes possible • good results	• low costs • mediocre results
Cons	• not for strong absorbing materials (steel, copper, …) • resolution size depends on sample size (mostly a few 10 µm³) • extremely high costs • time consuming • often not available	• surface roughness yields reduced values • only simple shapes feasible • precise weighing machine required	• precise weighing machine required • closed sample surface needed, porous samples are excluded	• slicing, grinding, and polishing required • high degree of uncertainty • obtained results often to high

Acknowledgements

The authors gratefully acknowledge funding by the German Research Foundation (DFG) within the Priority Program (SPP) 2122 “Materials for Additive Manufacturing (MATframe)” (grants NO462/13-1 and Re1261/23–1).

References

[1] Kaden et al., “Selective laser melting of copper using ultrashort laser pulses”, Applied Physics A, 123, 596 (2017).
[2] Ullsperger et al., “Selective laser melting of hypereutectic Al-Si40-powder using ultra-short laser pulses”, Applied Physics A, 123, 798 (2017).
[3] Yürekli et al., “Additive manufacturing of binary Al-Li alloys” Procedia CIRP, 94, 69-73 (2020).
[4] Kaden et al., “Additive manufacturing of pure copper using ultrashort laser pulses”. Proc. SPIE 10909, Laser 3D Manufacturing VI,109090D, doi: 10.1117/12.2507401.